

## Research Article

# Preparation, Mechanical, and Thermal Properties of Biodegradable Polyesters/Poly(Lactic Acid) Blends

Peng Zhao,<sup>1,2</sup> Wanqiang Liu,<sup>3</sup> Qingsheng Wu,<sup>1,2</sup> and Jie Ren<sup>1,3,4</sup>

<sup>1</sup>The Institute for Advanced Materials and Nano Biomedicine, Tongji University, Shanghai 200092, China

<sup>2</sup>Department of Chemistry, Tongji University, Shanghai 200092, China

<sup>3</sup>Institute of Nano and Bio-Polymeric Materials, School of Material Science and Engineering, Tongji University, Shanghai 200092, China

<sup>4</sup>Key Laboratory Advanced Civil Engineering Materials, Tongji University, Ministry of Education, Shanghai 200092, China

Correspondence should be addressed to Jie Ren, renjie.tongji@gmail.com

Received 30 September 2009; Accepted 27 November 2009

Academic Editor: Huisheng Peng

Copyright © 2010 Peng Zhao et al. This is an open access article distributed under the Creative Commons Attribution License, which permits unrestricted use, distribution, and reproduction in any medium, provided the original work is properly cited.

Series of biodegradable polyesters poly(butylene adipate) (PBA), poly(butylene succinate) (PBS), and poly(butylene adipate-co-butylene terephthalate) (PBAT) were synthesized successfully by melt polycondensation. The polyesters were characterized by Fourier transform infrared spectroscopy (FTIR), <sup>1</sup>H-NMR, differential scanning calorimetry (DSC), and gel permeation chromatography (GPC), respectively. The blends of poly(lactic acid) (PLA) and biodegradable polyester were prepared using a twin screw extruder. PBAT, PBS, or PBA can be homogeneously dispersed in PLA matrix at a low content (5–20 wt%), yielding the blends with much higher elongation at break than homo-PLA. DSC analysis shows that the isothermal and nonisothermal crystallizabilities of PLA component are promoted in the presence of a small amount of PBAT.

## 1. Introduction

In recent years, considerable interest has been focused on biodegradable polymers due to their obvious environment-friendly property comparing to conventional nondegradable or slowly degradable synthetic petrochemical-based polymeric materials [1, 2]. Biodegradable polymers degrade in a physiological environment by macromolecular chain scission into smaller fragments, and ultimately into simple stable end-products [3]. The degradation may occur via different pathway, such as catalysis of aerobic or anaerobic microorganisms, biologically active processes (e.g., enzyme reactions), and hydrolytic cleavage [4]. Poly(lactic acid) (PLA) is the most important plastic derived from renewable resources [5]. PLA-based products (e.g., NatureWork) have been extensively used for their application in biomedical field [6]. However, disadvantages of PLA are inherent brittleness and low toughness despite high tensile modulus and strength [7]. The flexibility, toughness and melt stability of PLA can be improved by some approaches, such as copolymerization [8, 9], blending [10], and plasticizers addition [11, 12]. Generally, blending is a relatively simple and easy way compared

to other approaches. Therefore, in recent years the blends of PLA and biocompatible and biodegradable polymers, such as poly( $\epsilon$ -caprolactone) (PCL) [13], poly(ethylene glycol) (PEG) [14, 15], poly(hydroxy butyrate) (PHB) [16], starch [17], poly(propylene carbonate) (PPC) [18], collagen [19], and PBS [20], have been widely studied for application in drug delivery and tissue engineering. PLA is approved for human use by the US Food and Drug Administration. Biodegradable polymeric nanoparticles (NPs) can be formulated to encapsulate various types of therapeutic agents including low-molecular-weight drugs, and macromolecules such as proteins or plasmid DNA. The NPs not only target the drug to its site of action but also maintain the drug concentrations at therapeutically relevant levels for a sustained period of time [21–23].

In this study, series of biodegradable polyesters, that is aliphatic homopolyesters PBA, PBS, and aliphatic-aromatic copolyester PBAT were synthesized by melt polycondensation. The blends of PLA and these biodegradable polyesters were prepared using a twin screw extruder. The mechanical and thermal properties of the blends were investigated.

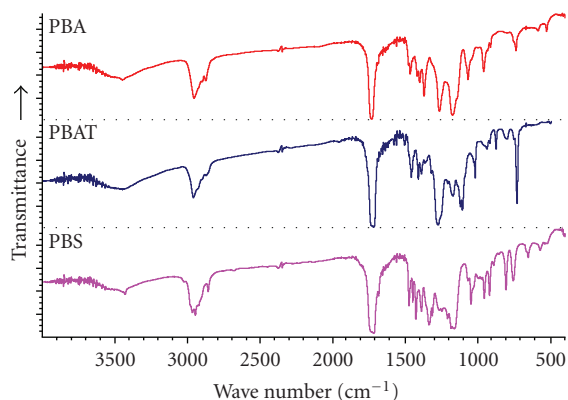


FIGURE 1: FTIR spectra of PBS, PBAT, and PBA.

## 2. Experimental

**2.1. Materials.** 1,4-butanediol, adipic acid and succinic acid (BASF, Germany), dimethyl-terephthalate (DMT, Merck), and tetrabutylorthotitanate (TBOT, Aldrich) were used without further purification. Pellets of PLA ( $M_w = 130,000$  g/mol) were purchased from Tongjieliang Biomaterials Co., Ltd., Shanghai, China. Other solvents used were purchased from the Shanghai Chemical Reagent Company, China Medicine (Group).

**2.2. Synthesis of Biodegradable Polyesters.** The homo- and copolyesters were synthesized by melt polycondensation of 1,4-butanediol, adipic acid and succinic acid, and DMT with TBOT as the catalyst.

The homopolyesters were prepared via a two-step process, that is, esterification first and subsequent polycondensation. Amount of adipic acid or succinic acid and 1,4-butanediol with designed mole ratio (1 : 1.2) were added into a 36 L stainless steel reactor under  $N_2$  atmosphere. The temperature of reactants was raised to  $160^\circ C$  with stirring, and the water formed during this reaction was removed by distillation. After reaction for 1–2 hours, a certain amount of TBOT was added to the reaction mixture under  $N_2$  atmosphere. Then the reaction temperature was raised from  $160^\circ C$  to  $230^\circ C$  within 5 hours under vacuum. After distillation of excess 1,4-butanediol, the reaction was carried out for another 20 hours under high vacuum ( $<50$  Pa).

The procedure of synthesis of copolyester PBAT was as follows: amount of adipic acid and 1,4-butanediol with designed mole ratio (1 : 1.2) were added into a 36 L stainless steel reactor under  $N_2$  atmosphere. The temperature of reactants was raised to  $160^\circ C$  with stirring, and the water formed during this reaction was removed by distillation. After reaction for 1–2 hours, TBOT was added to the reaction mixture under  $N_2$  atmosphere. The reaction temperature was raised to  $180^\circ C$  for 4 hours under vacuum. DMT, 1,4-butanediol, and TBOT with designed mole ratio (1 : 1.2) were added to the reaction mixture under  $N_2$  atmosphere. The reaction temperature was maintained at  $180^\circ C$  for 2 hours, and was then raised to  $230^\circ C$  within 4 hours under

vacuum. The reaction carried out for another 20 hours under high vacuum ( $<50$  Pa).

**2.3. Preparation of Polyesters/PLA Blends.** PLA and PBAT (PBS or PBA) were dried under a vacuum at  $45^\circ C$  for 12 hours to ensure that they were moisture free before being used. Blending of PLA and PBAT/PBS/PBA was performed using a corotating twin screw extruder (Leistritz ZSE-18) equipped with a volumetric feeder and a strand pelletizer. A screw with diameter of 27 mm and an L/D ratio of 40 were employed. The two polymers were weighed, manually tumbled to premix the pellets, and then fed into the extruder for melt blending. The extrusion temperature was independently controlled in eight zones along the extruder barrel and a strand die to achieve a temperature profile ranging from  $150^\circ C$  to  $180^\circ C$ . A 150 rpm screw speed was used for all extrusions. The blends obtained were cut into small pieces and dried at  $60^\circ C$  for 12 hours under vacuum before injection molding. The weight ratios of PLA/PBAT (PBS or PBA) were 95/5, 90/10, 85/15, 80/20, and 75/25.

**2.4. Characterization.**  $^1H$ NMR spectra were recorded on a Varian MERCURYPLUS400 Spectrometer with a  $CDCl_3$  signal as a standard. The thermal properties of the polymers were measured with a TA MDSC-Q100 differential scanning calorimeter with a heating rate of  $10^\circ C/minute$ . FTIR spectra in the range of  $4000\text{--}400$   $cm^{-1}$  were recorded on KBr pellet samples, with a Nicolet NEXUS-912A Spectrometer with a resolution of  $1$   $cm^{-1}$ . The molecular weight and the distribution of the polymers were measured by GPC (Waters150C). Tetrahydrofuran (THF) is used as the mobile phase at a flow rate of 1.0 mL/minute. Calibration is performed with polystyrene standards to determine the weight-average and number-average molecular weights ( $M_w$  and  $M_n$ ). Field emission-scanning electronic microscopy (FE-SEM) images of the multiblock copolymer samples were recorded on a FEI Quanta 200 FEG at an accelerated voltage of 15 kV. The samples were sputter coated with a thin layer of gold before observation.

Tensile tests and flexural tests were performed using an autograph tensile testing apparatus DXLL-5000 (Jiedeng Co., Ltd., China). The dumbbell-shaped specimens for tensile tests were prepared from compression molded samples according to the standard method for testing the tensile properties of rigid plastics (GB/T1040-1992). Span length was 50 mm, and the testing speed was 5 mm/minute. Specimens for flexural tests were also prepared from compression molded samples according to the standard of plastics (GB/T 9341-2000). Izod impact tests were carried out according to GB/T 16420-1996 standard, with a standard impact tester X CJ-50 (Chende Co., Ltd, China). Five composite specimens were tested for each sample, and the mean values and standard deviation were calculated.

## 3. Results and Discussion

**3.1. FTIR,  $^1H$  NMR and GPC.** Figure 1 shows FTIR spectra of PBS, PBAT, and PBA. The spectra show characteristic

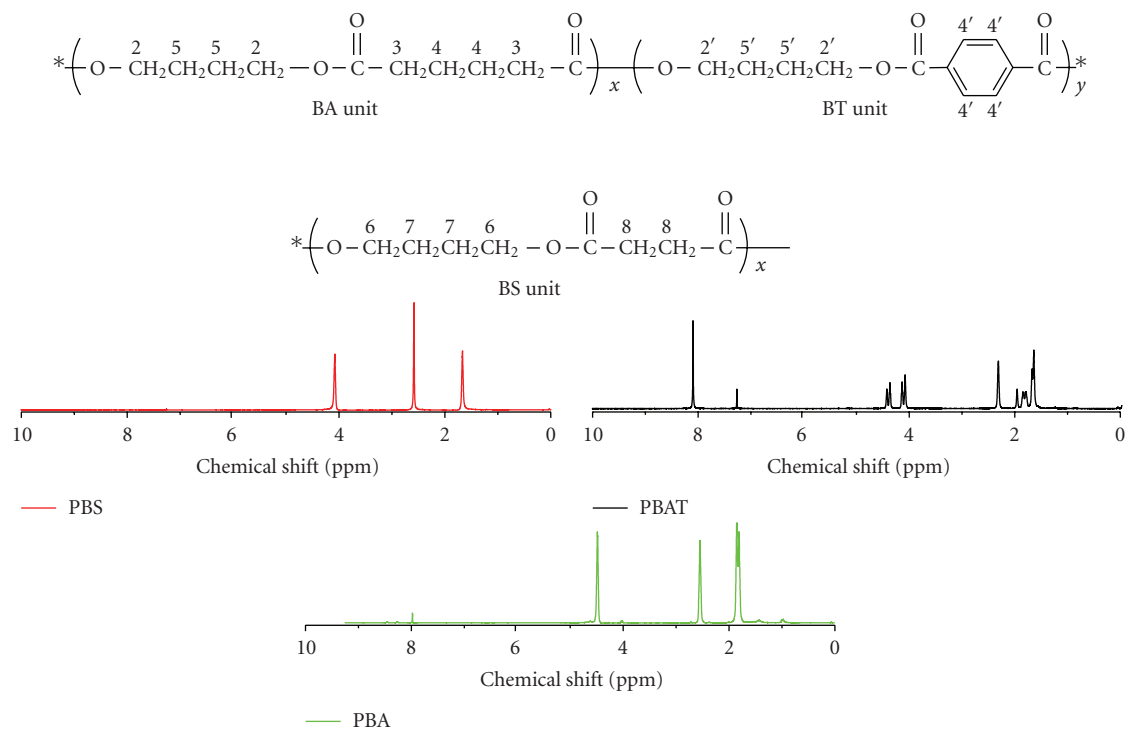


FIGURE 2:  $^1\text{H}$  NMR spectra of synthesized polyester.

ester absorption peaks at  $1690$ ,  $1670$ , and  $1725\text{ cm}^{-1}$  for the stretching vibration of the  $-\text{COO}-$  and at  $1100 \sim 1300\text{ cm}^{-1}$  for the stretching vibration of the  $\text{C-O-C}$ . In the FTIR spectrum of PBAT, the absorption bands at  $1018$ ,  $1456$ ,  $1495.65$ , and  $1573.91\text{ cm}^{-1}$  are characteristic group stretching of phenylene group. The red shift of ester absorption peak in PBAT is caused by conjugative effect between phenylene and carboxyl group.

Figure 2 shows  $^1\text{H}$  NMR spectra of these polyesters and corresponding proton resonance signals, respectively. The signals occurring at  $4.077$ ,  $2.314$ ,  $1.682$ , and  $1.643\text{ ppm}$  can be assigned to the methylene protons  $\text{H}_2$ ,  $\text{H}_3$ ,  $\text{H}_5$ , and  $\text{H}_4$ . The ratio of integrated peak area of  $\text{H}_2 : \text{H}_3 : (\text{H}_5 + \text{H}_4)$  is  $1 : 1 : 2$ , corresponding to those of BA unit in equimolar ratio. No  $\text{COOH}$  resonance signal can be detected due to instrumental detection limit. These data indicate that synthesized linear PBA chains are terminated by hydroxyl functional end groups. In  $^1\text{H}$  NMR spectrum of PBAT, the signal of aromatic protons appearing at  $8.10\text{ ppm}$  ( $\text{H}_4$ ) indicates phenylene structure in the polymer's chain. The signal of  $\text{CH}_2$  proton groups of BA unit appears at  $\delta$   $4.149$ ,  $4.091\text{ ppm}$ , and  $2.239\text{ ppm}$  ( $\text{H}_2$ ,  $\text{H}_3$ ) as a multiple peak; the ratio of the integrated peak intensities of  $\text{H}_2 : \text{H}_3$  is  $1 : 1$  corresponding to the molar ratio of hydrogen atoms ( $4 : 4$ ). The chemical shifts at  $\delta$   $4.436$ ,  $4.379\text{ ppm}$  for  $-\text{OCH}_2-(\text{H}'_2)$ , and  $\delta$   $8.097\text{ ppm}$  for proton adjacent to aromatic carbon ( $\text{H}'_4$ ) are attributed to those of BT unit. The ratio of the integrated peak intensities of  $\text{H}_3$  protons and  $\text{H}'_4$  protons is  $1.34 : 1$ , indicating that the content of BA unit is  $57.3\text{ mol}\%$ . The  $^1\text{H}$  NMR data are consistent with the proposed molecular structure of the polyesters.  $^1\text{H}$  NMR

TABLE 1: GPC and thermal characteristics of synthesized PBAT, PBS, and PBA.

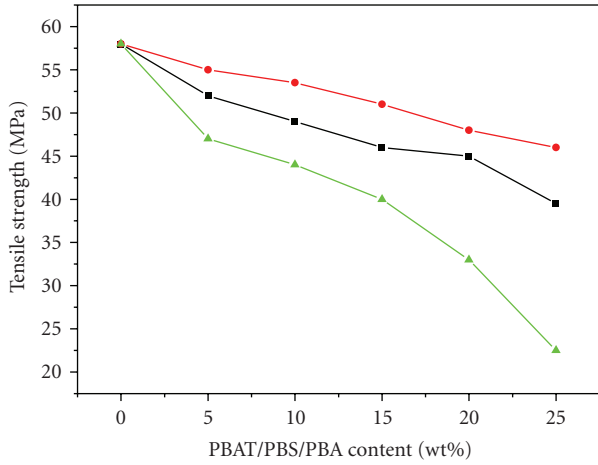
Sample	$M_w$	$M_n$	PI	$T_g$ ( $^{\circ}\text{C}$ )	$T_m$ ( $^{\circ}\text{C}$ )
PBAT	135000	59730	2.26	$-28$	114
PBS	98240	54270	1.81	$-36$	114
PBA	105000	57600	1.82	$-68$	55

spectrum of PBS shows three proton signals of BS unit, that is  $\delta$   $4.077$  for the proton of  $\text{H}_6$ ,  $\delta$   $1.673\text{ ppm}$  for  $\text{H}_7$ ,  $\delta$   $2.583\text{ ppm}$  for  $\text{H}_8$ . The molar ratio of structures  $\text{H}_6 : \text{H}_7 : \text{H}_8$  is approximately equal to  $1 : 1 : 1$ . All above data indicate that biodegradable polyesters of PBS, PBAT and PBA were synthesized successfully.

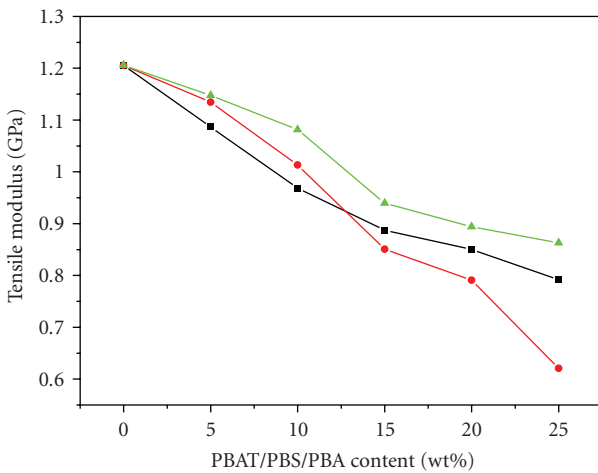
GPC results and thermal characteristics of PBAT, PBS and PBA are summarized in Table 1.  $M_w$  of PBAT, PBS and PBA are  $135000$ ,  $98240$  and  $105000$ , respectively, and  $M_n$  of PBAT, PBS and PBA are  $59730$ ,  $54270$  and  $57600$ , respectively. PDI are in the range of  $1.81-2.26$ .

### 3.2. Mechanical Properties

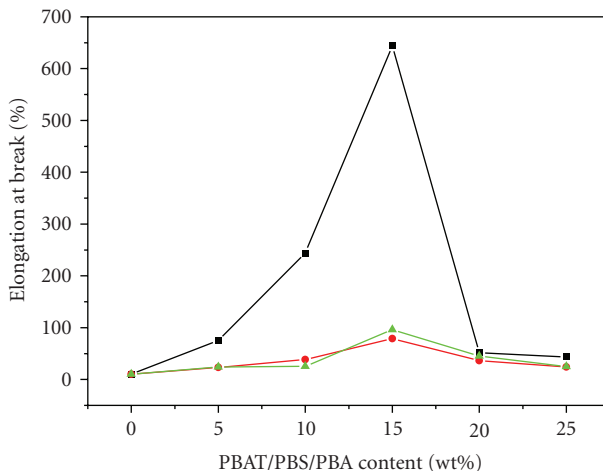
**3.2.1. Tensile Properties.** The tensile properties of PLA/PBS and PLA/PBA as well as PLA/PBAT blends are shown in Figure 3. The tensile strength and tensile modulus of PLA/PBAT (PBS, PBA) blends follow approximately the rule of mixtures over the whole composition range. Moreover, the PLA/PBAT blends showed much higher elongation at break than those of pure PLA and PLA/PBS and PLA/PBA blends over the whole composition range. Tensile strength



(a)



(b)



(c)

FIGURE 3: Tensile properties of PLA/PBAT and PLA/PBS, PLA/PBA blends: (a) tensile strength, (b) tensile modulus, and (c) elongation at break.

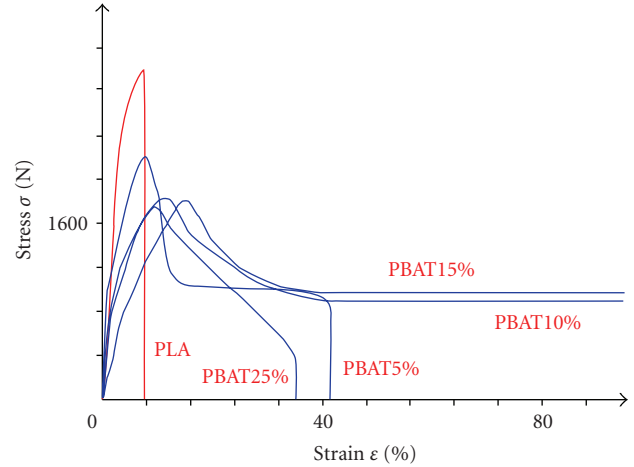


FIGURE 4: Stress-strain curves for PLA/PBAT 95/5, 90/10, 85/15, and 75/25 blends.

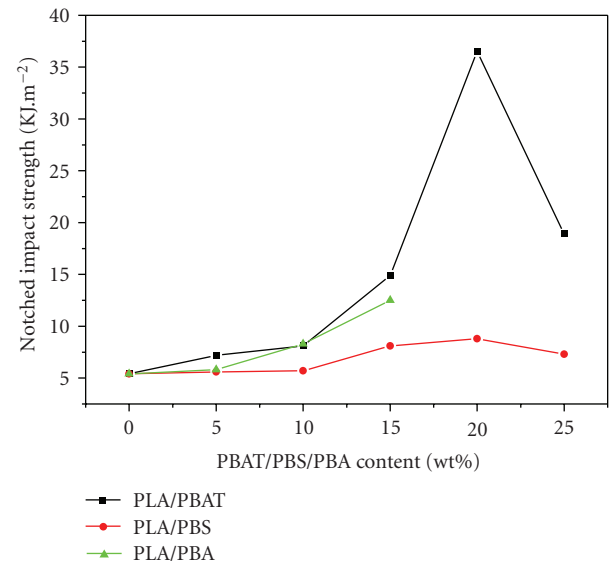


FIGURE 5: Notched impact properties of PLA/PBAT and PLA/PBS, PLA/PBA blends.

and Young's modulus of blends decreased with increasing polyester content, but elongation at break showed the peak values at 15 wt% of polyester content. Elongation at break (Figure 3(c)) increased with the increasing polyester content as expected. Small amount of polyester significantly alters the elongation. This is consistent with the tensile strength results. Addition of polyester to the PLA system resulted in a decrease in tensile strength and an increase in the elongation at break. The tensile strength of the blend did not significantly change with PBAT (PBS or PBA) content in the range from 5% to 15% but decreased rapidly when PBAT (PBS or PBA) content was increased to more than 25%. The elongation at break (Figure 3(c)) increased at higher polyester contents with the maximum value (>600%) occurring at a PBAT content of 15%. Interestingly, there is no dramatic decrease of tensile strength and modulus of the blends when polyester content

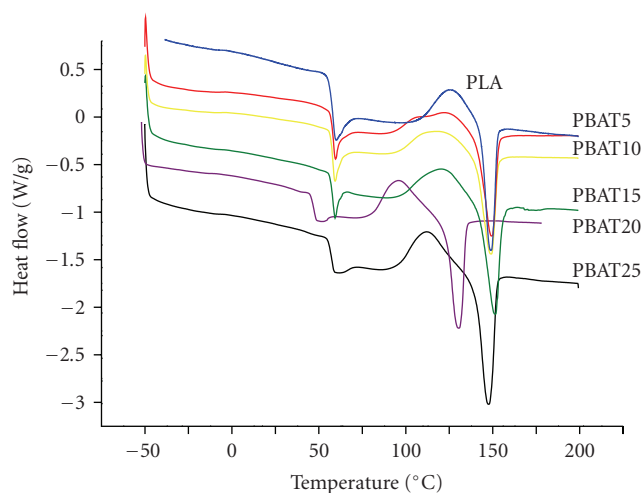


FIGURE 6: The DSC traces of PLA/PBAT blends.

was decreased to less than 20%. An increase of the polyester content to 15% does not lead to a significant decrease of the tensile strength and tensile modulus of the PLA/PBS (PBAT) blends. A decrease by 30% was observed for the PLA/PBA system.

It can be concluded from above analysis that the PLA/PBAT blends have the most outstanding properties. So the PLA/PBAT system was used for further investigation.

Figure 4 shows typical stress-strain curves for pure PLA and PLA/PBAT blends with different PBAT content. After a yield point, necking was observed. The necking continued until failure. Besides, strain hardening occurred after the yield point, and continued until failure. Fracture behavior of the specimen in the tensile tests changes from brittle fracture of plain PLA to ductile fracture of the blends. This is demonstrated in the tensile stress-extension curves as shown in Figure 4. Plain PLA shows a distinct break point before yielding and its strain at break is only about 7.7%. On the contrary, all the blends show distinct yielding and stable necking in cold drawing. Notably, when 5% PBAT was added, the elongation of the blend is tremendously increased by 200%.

**3.2.2. Impact Property.** The correlation between the notched impact strength and the composition of the PLA/PBAT, PLA/PBS and PLA/PBA blends are shown in Figure 5. Figure 5 shows that notched impact strength of plain PLA is 5.1 KJ/m<sup>2</sup> but increased to 15.3 KJ/m<sup>2</sup> when the content of PBAT is 15 wt%, and the notched impact strength can be 37.3 KJ/m<sup>2</sup> when the content of PBAT is 20 wt%. Therefore, it can be concluded that the addition of PBAT into PLA can remarkably improve the toughness of PLA. It can also be seen from Figure 4 that there is a sharp increase in the toughness of PLA/PBAT blends when the content of PBAT is up to 20 wt%, which is a sign of brittle-to-tough transition. Impact toughness is also increased from 5.1 KJ/m<sup>2</sup> for pure PLA to 12.6 KJ/m<sup>2</sup> for PLA-15%PBA as shown in Figure 4. Moreover, the notched impact strength of PLA/PBA blends

is too high to break when the content of PBA is higher than 20 wt%. Notched impact strength of PLA/PBS blends has similar trends as PLA/PBAT blends with a little difference.

**3.2.3. Toughening Mechanism.** SEM micrographs of tensile section and impact section are shown in Figures 7 and 8. Neat PLA which had no necking in the tensile test showed a smooth longitudinal fracture surface without visible plastic deformation. PLA/PBAT (15%) blend had the highest elongation at break, and its matrix underwent tremendous plastic deformation in the stress direction (Figure 7(d)). In the two-phase system, PBAT evenly dispersed in PLA matrix (Figure 8(b)). Normally, debonding of the round PBAT particles from the PLA matrix under tensile stress may cause oval cavities and these cavities were formed at the interface between the PLA matrix and PBAT inclusions during tension when the stress was higher than the bonding strength. PBAT debonded from the PLA matrix at the interface, so cavities arose. Since PBAT has different elastic properties compared to PLA matrix, its particles served as stress concentrators under tensile stress. The voids caused by debonding altered the stress state in the PLA matrix surrounding the voids, and triaxial tension was locally released and shear yielding was allowed. In the debonding progress, PLA matrix strands between PBAT particles deformed more easily to achieve the shear yielding. This toughening mechanism is consistent with other systems [24, 25].

**3.3. Thermal Properties of PLA /PBAT Blends.** The thermal properties of PLA/PBAT blends were investigated by DSC. The second heating curves for melt-quenched samples were chosen in order to remove previous thermal history and to make  $T_g$  more clear and obvious. The determined data are listed in Table 2 and the typical DSC curves are shown in Figure 6. At the same time,  $T_g$  and  $T_m$  of the blends with different compositions were observed. There are glass transition platforms at 50–60 °C corresponding to  $T_g$  of PLA component on all the curves. (DSC traces are not presented for  $T_g$  of PBAT component at -40 °C, because the exothermic heat flow is too slow to be detected during the test process.) Additionally,  $T_g$  of blends did not change with PBAT contents in blends. This trend suggests that the PLA and PBAT are not thermodynamic compatible, especially with higher PBAT content. If they are compatible, both  $T_g$ s of PLA and PBAT will move to combine with each other, and  $T_g$  peaks should be weaker and wider after they are extruded.

As shown in Figure 6, the addition of PBAT to the PLA matrix resulted in weaker and wider crystallization peak (about 110 °C), which was present at a lower temperature. This suggests that blending of PBAT with PLA has an influence on crystallizability of PLA. Moreover,  $T_m$ s of blends (about 150 °C) are same with  $T_m$  of pure PLA, indicating that addition of PBAT into PLA has no effect on  $T_m$  of PLA.

With the increase of PBAT content in blends,  $\Delta H_c$  and  $\Delta H_m$  of blends increase firstly, reach the highest value when the PBAT content is 15 wt%, and then decrease. It has been frequently practiced that the degree of crystallinity of thermoplastic is determined by dividing an observed heat of



TABLE 2: Composition and thermal characteristics of the samples.

Sample	PLA/PBAT <sup>a</sup> (wt%)	$T_g^b$ (°C)	$T_c^b$ (°C)	$T_m^b$ (°C)	$\Delta H_c^b$ (Jg <sup>-1</sup> )	$\Delta H_m^b$ (Jg <sup>-1</sup> )	$X_c^c$ (%)
PLA	100/0	58.36	124.70	148.64	10.337	11.00	12.76
PBAT5	95/5	58.40	122.65	149.46	11.28	13.12	13.92
PBAT10	90/10	58.27	116.19	149.79	11.83	15.10	14.61
PBAT15	85/15	58.07	120.73	151.39	14.42	18.67	17.80
PBAT20	80/20	58.60	110.02	147.59	12.09	17.36	14.93
PBAT25	75/25	58.00	111.88	147.39	10.24	16.74	12.64

<sup>a</sup>Weight ratio of the blends.

<sup>b</sup>The glass transition temperatures ( $T_g$ ), the crystallization temperatures ( $T_c$ ), the melting temperatures ( $T_m$ ), crystallization enthalpies ( $\Delta H_c$ ), melting enthalpies ( $\Delta H_m$ ) were registered by DSC at a heating/cooling rate of 10 °C/min.

<sup>c</sup>The degree of relative crystallinity ( $X_c$ ) was calculated by dividing the observed  $\Delta H_m$  from the first heating trace by the theoretical value (81 Jg<sup>-1</sup>) for a 100% crystalline PLA.  $X_c = \Delta H_c / \Delta H_c^* \Delta H_m^* = 81 \text{ J} \cdot \text{g}^{-1}$ .

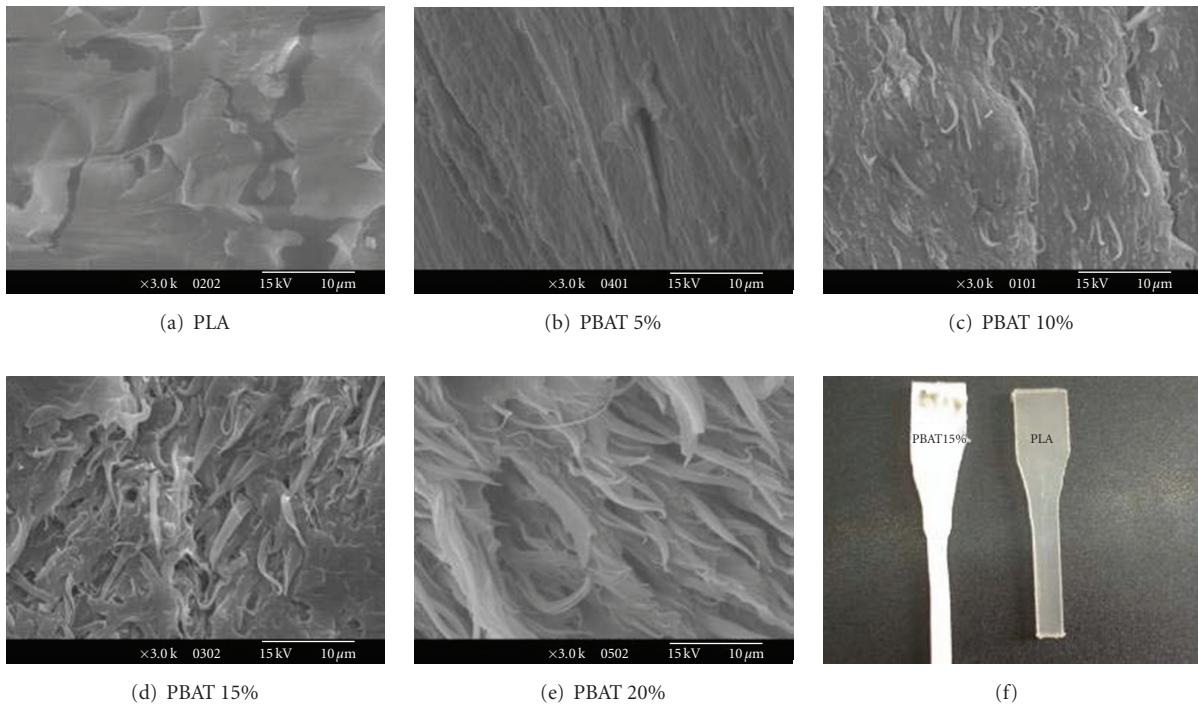


FIGURE 7: Tensile section SEM images of PLA/PBAT blends.

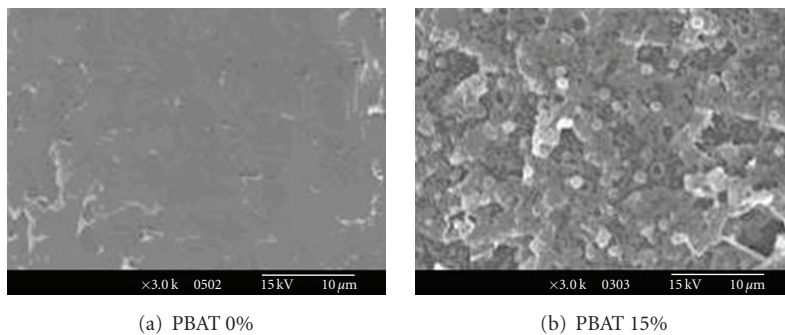


FIGURE 8: Impact section SEM images of PLA/PBAT blends.

fusion from the first heating trace by the theoretical value for a 100% crystalline polymer [26]. The theoretical  $\Delta H_m$  value for PLA was  $81 \text{ Jg}^{-1}$ . The data of  $X_c$  are listed in Table 2. The trend of  $X_c$  with the increase of PBAT content is the same as that of  $\Delta H_m$ . Therefore, the thermal properties of PLA, especially  $T_g$  and  $T_m$ , are slightly affected by the addition of PBAT. However, the addition of tough polyester to PLA matrix can influence the crystallizability of PLA matrix evidently.

#### 4. Conclusion

Biodegradable polyesters, that is, poly(butylene adipate) (PBA), poly(butylene succinate) (PBS), and poly(butylene adipate-co-butylene terephthalate) (PBAT), were successfully synthesized by melt polycondensation. These polyesters/PLA blends show considerably higher elongation at break than pure PLA with an acceptable loss of strength. The elongation at break increases at the higher polyester contents with the maximum value (>600%) occurring at a PBAT content of 15%. Addition of PBAT into PLA may improve the toughness of PLA. Moreover, the crystallizability of PLA component of blends can be increased by the addition of a small amount of PBAT.

#### Acknowledgments

The work is sponsored by the 863 High Technology Research and Development Program Plan of China (2006AA02Z248), the Program of Shanghai Subject Chief Scientist (07XD14029), the fund of Shanghai International co-operation of Science and Technology (no. 075207046) and the Shanghai Nano Special fund (0952nm04800).

#### References

- [1] E. Chiellini and R. Solaro, "Biodegradable polymeric materials," *Advanced Materials*, vol. 8, no. 4, pp. 305–313, 1996.
- [2] A. C. Albertsson and S. Karlsson, "Degradable polymers for the future," *Acta Polymerica*, vol. 46, no. 2, pp. 114–123, 1995.
- [3] D. J. Mooney, K. Sano, M. P. Kaufmann, et al., "Long-term engraftment of hepatocytes transplanted on biodegradable polymer sponges," *Journal of Biomedical Materials Research*, vol. 37, no. 3, pp. 413–420, 1997.
- [4] D. Satyanarayana and P. R. Chatterji, "Biodegradable polymers: challenges and strategies," *Journal of Macromolecular Science*, vol. C33, no. 3, pp. 349–368, 1993.
- [5] A. Torres, S. M. Li, S. Roussos, and M. Vert, "Poly(lactic acid) degradation in soil or under controlled conditions," *Journal of Applied Polymer Science*, vol. 62, no. 13, pp. 2295–2302, 1996.
- [6] E. T. H. Vink, K. R. Rábago, D. A. Glassner, and P. R. Gruber, "Applications of life cycle assessment to NatureWorks™ polylactide (PLA) production," *Polymer Degradation and Stability*, vol. 80, no. 3, pp. 403–419, 2003.
- [7] Y. Li and H. Shimizu, "Toughening of polylactide by melt blending with a biodegradable poly(ether)urethane elastomer," *Macromolecular Bioscience*, vol. 7, no. 7, pp. 921–928, 2007.
- [8] T. Ouchi and Y. Ohya, "Design of lactide copolymers as biomaterials," *Journal of Polymer Science A*, vol. 42, no. 3, pp. 453–462, 2004.
- [9] C. Nouvel, P. Dubois, E. Dellacherie, and J.-L. Six, "Controlled synthesis of amphiphilic biodegradable polylactide-grafted dextran copolymers," *Journal of Polymer Science A*, vol. 42, no. 11, pp. 2577–2588, 2004.
- [10] S.-Y. Gu, K. Zhang, J. Ren, and H. Zhan, "Melt rheology of polylactide/poly(butylene adipate-co-terephthalate) blends," *Carbohydrate Polymers*, vol. 74, no. 1, pp. 79–85, 2008.
- [11] M. Baiardo, G. Frisoni, M. Scandola, et al., "Thermal and mechanical properties of plasticized poly(L-lactic acid)," *Journal of Applied Polymer Science*, vol. 90, no. 7, pp. 1731–1738, 2003.
- [12] N. Ljungberg and B. Wesslen, "The effects of plasticizers on the dynamic mechanical and thermal properties of poly(lactic acid)," *Journal of Applied Polymer Science*, vol. 86, no. 5, pp. 1227–1234, 2002.
- [13] L. Wang, W. Ma, R. A. Gross, and S. P. McCarthy, "Reactive compatibilization of biodegradable blends of poly(lactic acid) and poly( $\epsilon$ -caprolactone)," *Polymer Degradation and Stability*, vol. 59, no. 1–3, pp. 161–168, 1998.
- [14] S. Tanoue, A. Hasook, Y. Iemoto, and T. Unryu, "Preparation of poly(lactic acid)/poly(ethylene glycol)/ organoclay nanocomposites by melt compounding," *Polymer Composites*, vol. 27, no. 3, pp. 256–263, 2006.
- [15] M. Sheth, R. A. Kumar, V. Davé, R. A. Gross, and S. P. McCarthy, "Biodegradable polymer blends of poly(lactic acid) and poly(ethylene glycol)," *Journal of Applied Polymer Science*, vol. 66, no. 8, pp. 1495–1505, 1997.
- [16] L. L. Zhang, C. D. Xiong, and X. M. Deng, "Biodegradable polyester blends for biomedical application," *Journal of Applied Polymer Science*, vol. 56, no. 1, pp. 103–112, 1995.
- [17] J.-F. Zhang and X. Z. Sun, "Mechanical and thermal properties of polydactic acid/ starch blends with dioctyl maleate," *Journal of Applied Polymer Science*, vol. 94, no. 4, pp. 1697–1704, 2004.
- [18] X. F. Ma, J. G. Yu, and N. Wang, "Compatibility characterization of poly(lactic acid)/ poly(propylene carbonate) blends," *Journal of Polymer Science B*, vol. 44, no. 1, pp. 94–101, 2006.
- [19] X. Q. Yang, M. L. Yuan, W. Li, and G. Y. Zhang, "Synthesis and properties of collagen/polylactic acid blends," *Journal of Applied Polymer Science*, vol. 94, no. 4, pp. 1670–1675, 2004.
- [20] W. P. Jun and I. Seung, "Phase behavior and morphology in blends of poly(L-lactic acid) and poly(butylene succinate)," *Journal of Applied Polymer Science*, vol. 86, pp. 647–655, 2002.
- [21] O. Zelphati, Y. Wang, S. Kitada, J. C. Reed, P. L. Felgner, and J. Corbeil, "Intracellular delivery of proteins with a new lipid-mediated delivery system," *Journal of Biological Chemistry*, vol. 276, no. 37, pp. 35103–35110, 2001.
- [22] J. Panyam and V. Labhasetwar, "Sustained cytoplasmic delivery of drugs with intracellular receptors using biodegradable nanoparticles," *Molecular Pharmacology*, vol. 1, no. 1, pp. 77–84, 2004.
- [23] S. Prabha and V. Labhasetwar, "Nanoparticle-mediated wild-type p53 gene delivery results in sustained antiproliferative activity in breast cancer cells," *Molecular Pharmacology*, vol. 1, no. 3, pp. 211–219, 2004.
- [24] G.-M. Kim and G. H. Michler, "Micromechanical deformation processes in toughened and particle filled semicrystalline polymers—part 2: model representation for micromechanical deformation processes," *Polymer*, vol. 39, no. 23, pp. 5699–5703, 1998.

- [25] K. Wang, J. S. Wu, L. Ye, and H. M. Zeng, "Mechanical properties and toughening mechanisms of polypropylene/barium sulfate composites," *Composites A*, vol. 34, no. 12, pp. 1199–1205, 2003.
- [26] Y. Yoo, M.-S. Ko, S.-I. Han, T.-Y. Kim, S. Im, and D.-K. Kim, "Degradation and physical properties of aliphatic copolyesters derived from mixed diols," *Polymer Journal*, vol. 30, no. 7, pp. 538–545, 1998.





**Hindawi**

Submit your manuscripts at  
<http://www.hindawi.com>

